An Investigation of the Effects of Media Characteristics on Read Channel Performance for Patterned Media Storage

Paul W. Nutter, *Member, IEEE*, Ioannis T. Ntokas, *Student Member, IEEE*, and Barry K. Middleton, *Member, IEEE*

School of Computer Science, The University of Manchester, Manchester M13 9PL, U.K.

Many view data storage on patterned magnetic media as one way of attaining storage densities in excess of 1 Tb/in^2 and thus overcoming the problems associated with recording at ultrahigh densities on conventional continuous media. In this paper we investigate, through the use of a replay simulation developed to take into account the three-dimensional nature of the patterned media, the effects that the shape-constrained media have on the bit-error-rate performance of the read channel in 1-Tb/in^2 perpendicular recording. In particular, we analyze how media configurations with varying island shape, size, and distribution affect the channel performance.

Index Terms—**Generalized partial response, patterned media, perpendicular recording, shape constrained media.**

I. Introduction

ADVANCES in the data capacities of magnetic storage systems have only been possible through the continued refinement of both the storage media and the recording and replay properties of the heads. Current commercial systems employ longitudinal magnetic media, where the direction of magnetization lies in the plane of continuous magnetic film. It is envisaged that future generations of magnetic recording systems will increasingly employ perpendicular media, where the direction of magnetization lies perpendicular to the plane of the film; in this arrangement, improved storage capabilities have been observed compared to longitudinal media [1]. The move to perpendicular media has posed a number of technical challenges; most notably, the need for single-pole recording heads, the fabrication of a thin-film perpendicular media on soft magnetic underlayers (SULs), and the development of new read channel designs due to the signal spectra differences between longitudinal and perpendicular systems [2]. All of these challenges have been successfully addressed and made the realization of commercial perpendicular drives possible. However, beyond perpendicular media, many believe the use of patterned media will be essential [3]–[5] in order to achieve storage densities in excess of 1 Tb/in^2 and overcome the physical barriers that restrict ultrahigh-storage densities in continuous media. Such a paradigm shift will undoubtedly introduce further technical difficulties that must be overcome in order to realize practical storage systems; not least, the problems associated with the fabrication of media.

In patterned media based storage systems, single bits of data are recorded to discrete, nanometer-sized lithographically defined islands, each being (ideally) single domain. The size, shape, and distribution of these islands depends on the fabrication process adopted, which is under the control of media designers. The main advantage of patterned media over conventional media using continuous magnetic thin films is the ability to circumvent the superparamagnetic limit. In a magnetic storage system, the signal-to-noise ratio (SNR) is related to the number of magnetic grains per recorded bit. A reduction in recorded bit size requires a reduction of the grain size in order to retain a sufficient number of grains per bit and maintain an acceptable SNR. However, as grain sizes are reduced they become less thermally stable, to such a degree that data storage is no longer viable [6]. In the case of patterned media, the grains forming the magnetic islands are strongly coupled and, as a result, do not require any grain size reduction [7]–[9]. In addition, due to the nonmagnetic region between islands, transition noise, which is prevalent in continuous thin-film based media, is effectively removed [6], [10]. The nonmagnetic region between tracks also permits the removal of side tracks which exist in continuous film based media to ensure sufficient separation between recorded tracks; this also permits the possibility of "built-in" tracking capabilities [6].

In this paper, we will examine how the geometry and distribution of the patterned islands, i.e., island length, size, and period, affect the performance of the read channel in terms of bit-error rate (BER) against SNR and hence determine the best media configuration to offer optimum read channel performance. In addition, other media characteristics, such as film thickness and the presence of an SUL, will be investigated. In order to facilitate this work, a readout simulation has been developed which takes into account the three-dimensional (3-D) nature of patterned media and accurately predicts the replay waveforms as functions of the media characteristics. In addition, the 3-D readout simulation also predicts signal contributions arising due to inter-track-interference (ITI) in the readout waveform. In order to determine the data recovery performance, a partial-response maximum-likelihood (PRML) read channel simulation has also been developed. The simulation will be used to assess the performance of a range of common partial-response (PR) targets applicable for use in patterned media storage systems.

Patterned media read channel and write designs have been analyzed previously by Hughes [11]–[14] for 100-Gb/in^2 media [11], [12] and later 1-Tb/in^2 media [13], [14] with and without an SUL. The work presented here concentrates on 1-Tb/in^2 storage densities and enhances understanding (concentrating on read channel designs only) in a number of areas:

Digital Object Identifier 10.1109/TMAG.2005.856586

by using a 3-D model of the replay process as compared to the two-dimensional (2-D) approaches of Potter [15] and Ruigrok [16], which more accurately predicts the potential distribution beneath the giant-magnetoresistive (GMR) read head in the presence of an SUL; by introducing the more realistic case of ITI in the replay waveform; by analyzing how the island geometry, period, bit-aspect ratio (BAR), and distribution affects the read channel BER performance; by more accurately modeling the effects of lithography jitter taking into account both shifts in the island position [11] and variation in the size of the islands; by using a full channel simulation (Monte Carlo analysis), which models all the read channel components and generates the BER by calculating data in error at the output of the read channel, rather than using analytical approaches; and by analyzing a PRML read channel incorporating an optimized generalized-partial-response (GPR) polynomial.

The paper is organized as follows. Section II describes the 3-D modeling approach used to simulate replay waveforms in patterned media storage systems. Section III describes the channel simulation and the use of GPR targets used in the analysis. Section IV presents analysis results, and conclusions are summarized in Section V.

II. Replay Simulation

In a previous paper [10], we demonstrated that the shape of the replay pulse due to an isolated island (along-track), using a conventional shielded GMR reader, is strongly dependent on the magnetic film structure and the geometry of the patterned island. There, the replay simulation took into account the 3-D geometry of the patterned islands through an extension of the reciprocity integral to 3-D.

Traditional signal modeling techniques based on the reciprocity integral [15], [16] assume that the medium magnetization is uniform across-track (infinite width approximation). However, in the case of patterned media, this is not the case, and a more accurate replay model would need to take into the account the geometrical constraints of the patterned media in both the along-track and across-track directions beneath the replay sensor. The approach used is described in detail in [10] and is summarized briefly below.

Fig. 1 illustrates the geometry of the shielded GMR head and the patterned magnetic medium. Here, the GMR element is of track width W, and length (along-track) L, the side shields are of infinite extent across-track, of semi-infinite height and separated from the GMR element by gaps of width G. The islands (assumed to be square in cross section unless otherwise stated) are arranged in a square array and have length a, and period x_b (in distance), which is equal along and across-track. The head scans in the direction x, at a velocity v.

The signal flux through the GMR read sensor, due to magnetization changes in the medium, can be calculated using the standard reciprocity integral

$$\Phi_{\rm sig}(\bar{x}) = \mu_o \int_{-\infty}^{\infty} \left[\int_{d}^{d+\delta} -\frac{\partial \phi(x,y)}{\partial y} dy \right] M_y(x-\bar{x}) dx dz \quad (1)$$

where $\Phi_{\rm sig}$ is the signal flux though the sensor, M_y is the medium magnetization, which is assumed to be perpendicular and varying in the scan direction, x, only, and ϕ is the scalar magnetic potential distribution, at position y below the air-bearing surface (ABS) of the GMR head.

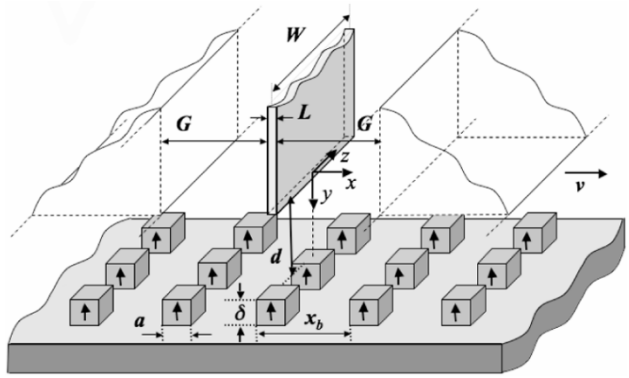

Fig. 1. Geometry of the shielded GMR head structure and patterned magnetic medium.

By adopting simple potential profiles across the gap of the GMR head, Potter and Ruigrok approximations [15], [16], the reciprocity integral of (1) can be easily evaluated. Extension of the reciprocity integral to 3-D gives

$$\Phi_{\rm sig}(\bar{x}) = \mu_o \int_{-\infty}^{\infty} \int_{-\infty}^{\infty} \left[\int_{d}^{d+\delta} \frac{\partial \phi(x,y,z)}{\partial y} dy \right] \times M_y(x-\bar{x},z)\, dx\, dz \quad (2)$$

where the variation in the medium magnetization, M_y, in both the along-track, x, and across-track, z, directions is taken into account and the scalar magnetic potential distribution, ϕ, is calculated across any 2-D plane below the ABS using the approach of Wilton [17]; in this case, the presence, or not, of any SUL is taken into account in the potential calculation.

The replay waveform due to a track of islands can be generated by either superposing pulse responses due to an isolated island or by superposing isolated step responses (nonmagnetic to magnetic material transitions) at the two edges of each island along the track. Following this approach, signal contributions (degradations) in the form of ITI arising due to read head pick-up from neighboring tracks can be easily included. Here, the signal contributions due to the adjacent tracks are generated using step responses produced with the read head offset across-track by a track pitch, x_b. The introduction of signal contributions due to adjacent tracks is not possible using conventional 2-D modeling approaches.

In the following analysis, the SNR is defined as

$$\mathrm{SNR(dB)} = 20 \log \left(V_{0-p} / v_{\rm rms} \right) \quad (3)$$

where V_{0-p} is the peak signal of the signal waveform due to a spread of random data and $v_{\rm rms}$ is the rms noise voltage, which is assumed to be additive white Gaussian (AWGN).

The other source of noise in patterned media storage systems is due to jitter arising from imperfections in the patterning process; this manifests itself as variations in island size and position and can be shown to be Gaussian in nature [18]. Jitter can be introduced as random transition shift in the step superposition process with Gaussian distribution of zero mean and vari-

ance σ_j^2, where σ_j is specified as a percentage of the bit period, x_b. The medium M_s is assumed to be constant.

III. Channel Simulation

A read channel simulation has been developed in order to predict the performance of the magnetic read channel, in terms of BER against system SNR. The complete system, including both replay and read channel simulations, is illustrated in Fig. 2.

The full read channel consists of a PRML decoder and a modulation decoder (if used). The PRML block consists of a 7-tap finite-impulse-response (FIR) digital filter followed by a maximum likelihood Viterbi decoder. The role of the FIR filter is to modify the spectrum of the replay waveform to match that of a desired PR target.

Generally, the choice of PR target used in magnetic recording is of the polynomial form $(1-D)(1+D)^n$, where D is the delay operator and n is an integer. The effect of the differential operator $(1-D)$ is to introduce a spectral null at dc which is required in longitudinal recording due to the lack of dc response. In perpendicular recording, the $(1-D)$ term is removed since the maximum signal level is observed at dc in the presence of an SUL of infinite permeability [19].

In general, integer valued PR targets do not offer a perfect spectral match to the channel response, particularly at high storage densities, in which case a target response with noninteger coefficients may be more appropriate [20]. Such GPR targets enable more accurate channel-spectrum matching and near-optimal white noise filtering [21] and have been shown to offer improved performance over conventional integer-valued PR targets, even in the presence of jitter noise [22]. The implementation of the Viterbi decoder will become more complex as a result of the noninteger PR coefficients; however, the performance gain may be significant [20].

Fig. 3 gives a detailed block diagram of the simulated read channel (dashed line indicates the filter optimization path). Here, the ideal channel data sequence, a_k, which may, or may not, be run-length-limited (RLL) encoded is passed through the channel model, which generates a replay waveform with the required noise, n_k, and jitter, Δ_k. The replay waveform is then sampled (ideally at positions in the replay waveform corresponding to the center of the islands along the main data track) at the channel data rate, $1/T_b$, where $T_b = x_b/v$, to produce the sampled signal data, s_k. The FIR filter, or equalizer, $F(D)$, is configured to produce a sampled output signal, c_k, that closely resembles samples, d_k, generated by a desired target, $G(D)$. The equalized data then passes through the Viterbi decoder from which the data is recovered.

The FIR filter coefficients, $F(D)$, are optimized in order to minimize the mean-squared-error (MSE) between the equalized channel samples, c_k, and the ideal target samples, d_k, generated by the desired target, $G(D)$. In the case of integer-valued PR targets, this is achieved using the least-mean-squared (LMS) algorithm. In the case of the GPR targets, both the filter coefficients, $F(D)$, and the target coefficients, $G(D)$, are found simultaneously [20], [22]; this process is summarized briefly below.

Let the GPR target polynomial be of length L with time-domain coefficients $\boldsymbol{G} = [g_0, g_1, \ldots, g_{L-1}]$, and the FIR filter polynomial be of length $N = 2K+1$ with time-domain coefficients $\boldsymbol{F} = [f_{-K}, f_{-K+1}, \ldots, f_{K-1}, f_K]$. Then following

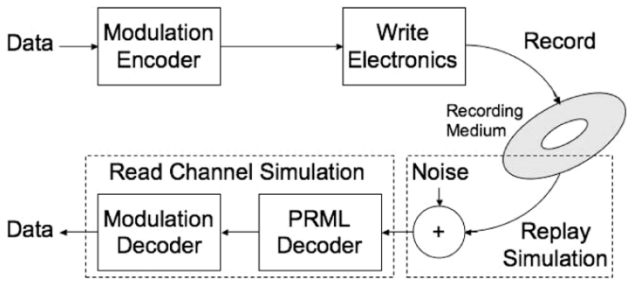

Fig. 2. Block diagram of the magnetic PRML read channel simulation.

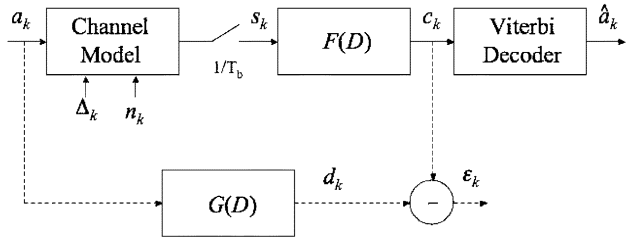

Fig. 3. Read channel block diagram (dotted line indicates the equalizer design block).

the monic constraint, $g_0 = 1$, which avoids the trivial solution $\boldsymbol{G} = \boldsymbol{F} = 0$ being reached, it can be shown that the minimum MSE is given by

$$\lambda = \frac{1}{I^T(A - M^T R^{-1} M)^{-1} I} \tag{4}$$

where λ is the Lagrange multiplier [22], T is a matrix transpose, $\boldsymbol{I}$ is an L-element column vector with first-element 1 and all other elements zero; $\boldsymbol{A}$ is an L-by-L auto-correlation matrix of the ideal channel data, a_k; $\boldsymbol{M}$ is an N-by-L cross-correlation matrix of the sampled data, s_k, and the ideal channel data, a_k; and $\boldsymbol{R}$ is an N-by-N auto-correlation matrix of the sampled data, s_k.

The optimum target time-domain coefficients for $\boldsymbol{G}$ and $\boldsymbol{F}$ are then given by

$$G = \lambda(A - M^T R^{-1} M)^{-1} I \tag{5}$$

$$F = R^{-1} M G \quad . \tag{6}$$

In this paper, an FIR filter of length $N = 7$ has been chosen while a GPR polynomial of length $L = 5$ has been adopted as this has been shown to be sufficient for improved channel performance in the case of perpendicular recording [21].

IV. Analysis

In the following analysis, a GMR read head with the fixed dimensions listed in Table I has been used. For these dimensions, the replay pulse due to an isolated square island of length 12.5 nm has a PW_{50} of 18.8 nm in the case of medium with no SUL (with track profile plot PW_{50} of 29.5 nm), and 21.2 nm in the case of a medium employing an SUL (with track profile plot PW_{50} of 31.2 nm); such dimensions should support storage densities in the order of 1 Tb/in^2.

Throughout the following analysis (unless otherwise stated), a perpendicular patterned medium with island length $a = 12.5$ nm (assumed square) and period $x_b = 25$ nm (along and across-track) has been assumed; the islands are ideal, i.e., no jitter, and

TABLE I
GMR HEAD DIMENSIONS

Dimensions (nm)	
Sensor width (W)	20
Sensor Length (L)	4
Shield-to-shield spacing ($L+2G$)	16

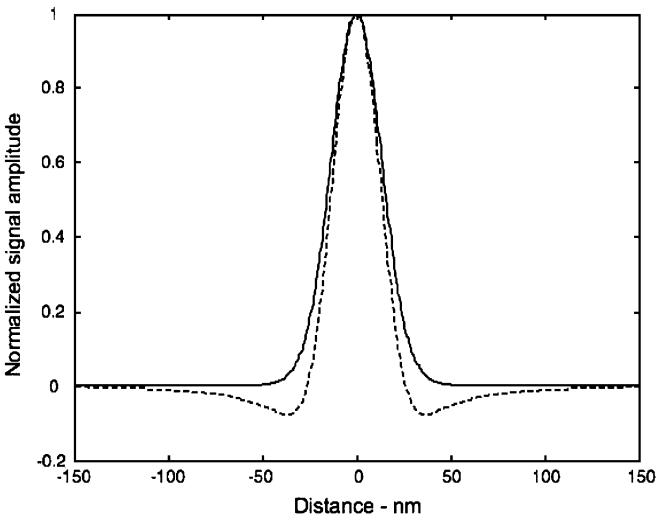

Fig. 4. Replay pulse response due to an isolated square island of length 12.5 nm, for an SUL present (solid line) and no SUL (dotted line).

are single domain. A fly height of $d = 10$ nm and film thickness of $\delta = 10$ nm have been adopted (unless otherwise stated).

Two media configurations have been analyzed in detail: a patterned medium without an SUL and a patterned medium employing an ideal SUL of infinite permeability. In the case of a patterned medium with an SUL, no interlayer between the bottom surface of the recording medium and the SUL has been assumed.

The shape of the replay pulse arising due to an isolated island is strongly dependent upon the presence, or not, of an SUL. In the case where the SUL is absent, the replay pulse is characterized by the presence of undershoots either side of the main pulse, as illustrated in Fig. 4, whereas in the SUL case, no undershoot is observed [10].

Fig. 5 illustrates plots of channel performance (in terms of BER against SNR) for the two media configurations of interest. BER curves are illustrated which have been generated using waveforms produced using both a conventional 2-D approach (Ruigrok) and the described 3-D replay simulation (3-D). In addition, in the case of the 3-D replay simulation, the BER performance in the presence of adjacent tracks is also illustrated (3-D-multi). In all cases, a GPR target has been used and optimized for a system SNR of 20 dB.

It is clear from Fig. 5 that the 2-D (Ruigrok) approach has a tendency to underestimate the channel performance; this is likely to be due to the increased undershoot evident in the replay pulse [10]. The use of the (more realistic) 3-D replay simulation indicates an improved channel performance. In the realistic case where adjacent tracks are introduced, which cannot be treated using the 2-D approaches, the ITI introduced by the read

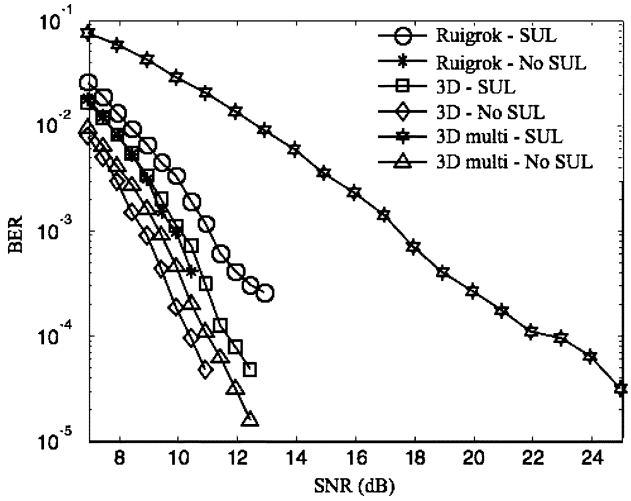

Fig. 5. Channel performance using an island length of 12.5 nm and period 25 nm.

head sensing the adjacent tracks results in a reduced BER performance. In the case of a medium employing an SUL, the degradation in channel performance is severe (the minimum SNR for an acceptable BER of 10^{-4} changes from 11.6 to 22.4 dB). However, in the case where these is no SUL, the effect is minimal (the minimum SNR changes from 10.4 to 11.0 dB for an acceptable BER of 10^{-4}).

The main point of interest from Fig. 5 is that to achieve optimum BER read channel performance a patterned medium without an SUL should be employed; this may benefit media designers due to the problems associated with patterning of the recording film while maintaining a continuous SUL film.

A. Choice of PR Target

In order to determine the optimum PR target (in terms of channel BER performance), a number of conventional PR schemes have been investigated, as well as the GPR target. The PR targets chosen are those used extensively in longitudinal recording, such as the PR4 family of targets (PR4, EPR4, EEPR4), as well as a PR5 target [23]; a similar target has already been investigated with respect to implementation in patterned media storage systems using longitudinal media [11]. The conventional PR4 targets have been investigated due to the fact that the channel response of the system has a reduced dc response similar to that of a longitudinal system; this arises due to the generation of a pulse in the replay waveform due to each individual island. In order to demonstrate the poor spectral matching to a PR scheme designed for perpendicular media, the PR$(-1, 0, 1, 1, 0, -1)$ target [24] was also investigated.

Fig. 6 illustrates the BER performance for the chosen PR targets using the two media configurations under investigation. In all cases, the signal contributions due to the adjacent tracks (ITI) have been included in the generation of the replay waveform.

In both plots, it is clear that the GPR target offers optimum performance compared to the other targets investigated. In the no SUL case, for an acceptable BER of $<10^{-4}$, a minimum SNR of 11 dB can be tolerated in the channel incorporating a GPR target. In the SUL case, using the GPR target the channel can tolerate a minimum SNR of 22 dB for a BER of $<10^{-4}$. It is also clear that a much better BER performance is observed

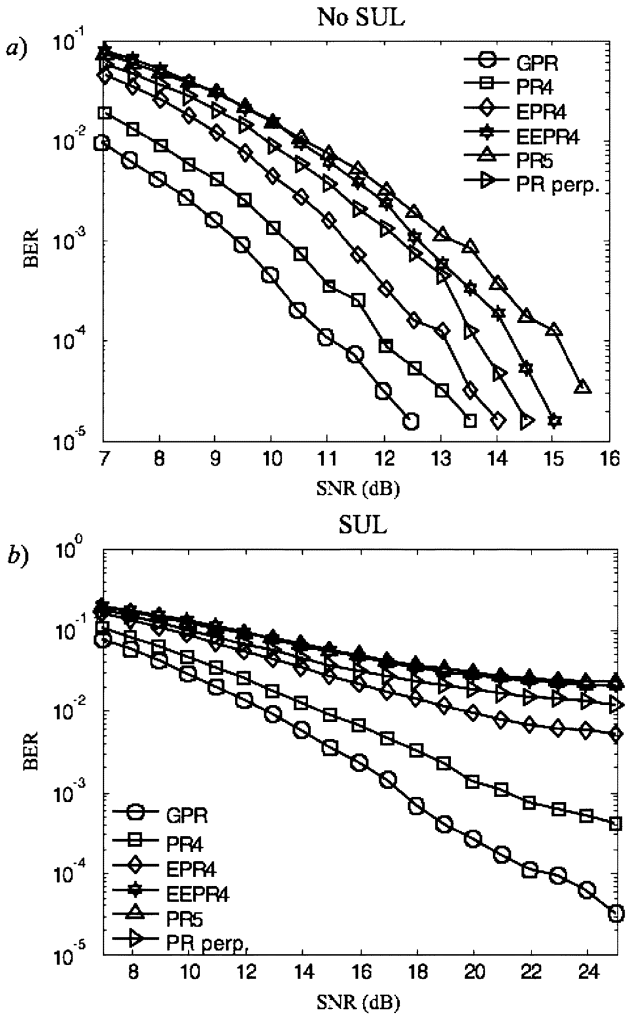

Fig. 6. Channel performance using different PR schemes, for the case of (a) no SUL, and (b) an SUL present.

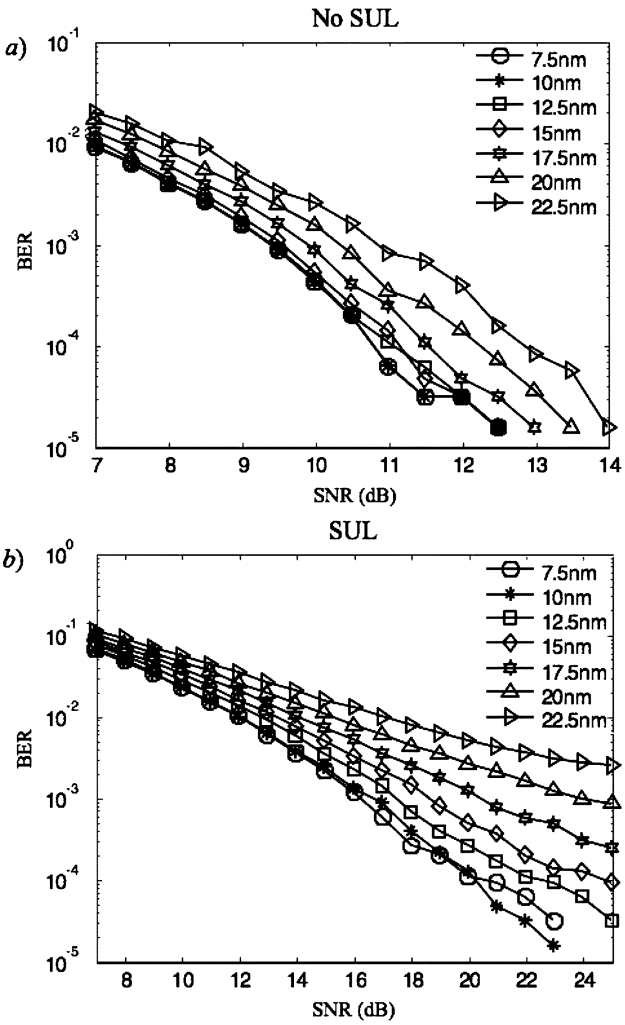

Fig. 7. Channel performance for varying island length, for the case of (a) no SUL, and (b) an SUL present.

using the PR4 and EPR4 targets, compared to the perpendicular PR target (PR perp.), as expected from the analysis of the channel spectrum. It is interesting that for the case where an ideal track of data is assumed where there is no ITI (not shown), then the optimized GPR target is similar to that of the dicode channel, $(1, -1)$, in both cases. The GPR polynomials used are $(1, -0.507, -0.496, 0.009, 0.0002)$ in the no SUL case and $(1, -0.409, -0.432, -0.048, -0.027)$ in the SUL case.

Throughout the following analysis, a GPR target will be assumed and optimized in each case for a system SNR of 20 dB unless otherwise indicated.

B. Dependence on Island Shape

In conventional continuous media, the storage density is determined by the BAR, i.e., the ratio of the track density to the linear bit density along track. Generally, a high BAR is desirable (of the order 10 in current commercial systems [25]) since increased track density results in increased media noise, particularly from the track edges [25]. In addition, in terms of recording, the write field falls off significantly as the pole width (and hence BAR) is reduced and there is also an inability to confine the fringe fields at very narrow tracks widths [26].

In the case of a patterned recording system, the shape, size, and distribution of the islands, and hence BAR, are determined primarily by the medium patterning process. For example, in the case of interference lithography, the resulting islands are generally distributed over a square array with the size and separation of the islands controlled by the fabrication process. In the case of e-beam lithography, there is more freedom to control the shape and distribution of islands. However, generally the patterning process produces square, or circular, islands, which implies a BAR of 1. Such a low BAR may not be such a disadvantage in patterned media systems due to the fact that track edge effects are effectively removed as a result of the patterning process that (ideally) confines the recorded mark to a single domain island. As such, the dominant source of noise as a consequence of reduced BAR will be the introduction of ITI due to the read head sensing the adjacent tracks.

Fig. 7 illustrates the BER performance of the read channel when the width of the (assumed rectangular) islands is varied, for the two media configurations being investigated. The length (along-track) and period (along and across-track) of the island are held fixed at 12.5 and 25 nm, respectively. It is worth noting that at the storage density of interest, there is little difference in channel BER performance when using round or square islands.

In both cases, it is clear that the channel BER performance is dependent upon the width of the islands. The degradation in channel performance as the island width is increased is due to the increased amount of ITI due to the islands along the adjacent tracks being located physically closer to the main data track as the width is increased. It can be shown that for an island width of infinite extent, compared to the width of the GMR read sensor, the BER performance is comparable to that determined using the (conventional) 2-D modeling approach. Again, this result is consistent with an analysis of the pulse shape due to an isolated island, which can be shown to approximate to the response generated using 2-D modeling approaches for large bit width (high BAR) [10]. When the width of the island is reduced below 12.5 nm, i.e., $x_b/2$, little appreciable improvement in BER performance is observed.

In the case where the island width is held fixed (at 12.5 nm) and the island length is increased, then very little change in channel BER performance is observed in the case where there is no SUL present (change in SNR of 1.5×10^{-5} at 12 dB) and some slight performance degradation in the case where an SUL is present (change in SNR of 2×10^{-4} at 22 dB). Overall, using the read head dimensions adopted, the effect of ITI is the main cause of reduced channel performance as the size of the island is changed (but the period remains fixed).

C. Dependence on Island Period

In the case where the island length/width is held fixed, the amount of inter-symbol-interference (ISI) in the replay waveform is determined by the separation between (or period of) the islands. Fig. 8 illustrates plots of channel BER performance when the island period is varied; here the length of the (assumed square) island is held fixed at 12.5 nm.

In both cases, the channel BER performance improves as the periodicity of the islands is increased; this result is sensible considering that the amount of ISI is reduced as the islands are physically located further away from each other. Conversely, reducing the period of the islands results in reduced channel performance due to increased ISI. It is clear from Fig. 8(b) that for the SUL case, it is difficult to push the storage density beyond 1 Tb/in^2 using the GMR head dimensions adopted. However, in the no SUL case, Fig. 8(a), the island period can be reduced to 20 nm, giving a storage density of 1.6 Tb/in^2, while maintaining a BER comparable with the SUL case at 1 Tb/in^2, i.e., a minimum SNR of approximately 22 dB for an acceptable BER of 10^{-4}.

D. Dependence on Island Distribution

In all the previous results, it has been assumed that the islands are distributed over a square array, i.e., the positions of the islands along the neighboring tracks are directly adjacent to those along the main data track. However, the arrangement of islands is dependent on the fabrication process. For example, island formation through resist masks produced by the self-assembly of nanometer sized polystyrene spheres results in islands packed over a hexagonal lattice [27]. In this case, the islands along neighboring tracks are no longer directly adjacent, but displaced half an island period, $x_b/2$, down track. As a result, any ITI at the data sampling point (the point in the replay waveform corresponding to the center of an island) will be reduced. We

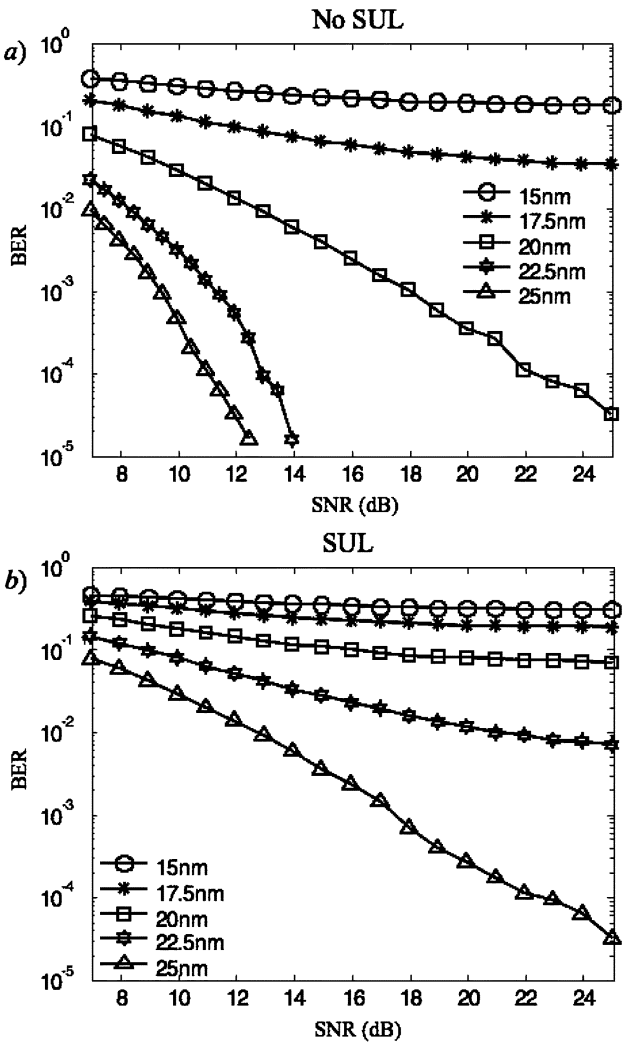

Fig. 8. Channel performance for varying island period (fixed island length of 12.5 nm), for the case of (a) no SUL, and (b) an SUL present.

have shown previously [28], that for a patterned medium with an SUL, the use of a hexagonally packed island distribution offers improved read channel BER performance as well as less sensitivity to track misregistration (TMR).

Fig. 9 illustrates the read channel BER performance for the cases of islands distributed on a square array and on a hexagonally packed lattice, for the two media configurations being investigated. The islands are assumed to be square and of length 12.5 nm and period along and across-track of 25 nm. In the case of a patterned medium with an SUL, Fig. 9(b), it is clear that the use of a hexagonally packed island distribution results in an improved channel BER performance, i.e., a change in minimum SNR of 22 to 15 dB for an acceptable BER of 10^{-4}. In the no SUL case, some improvement in BER performance is also observed.

E. Dependence on Film Thickness

The thickness of the medium can have an effect on the shape of the pulse response due to an isolated island, particularly in the case of a patterned medium with an SUL [10]. In both media configurations, a degradation in read channel BER performance

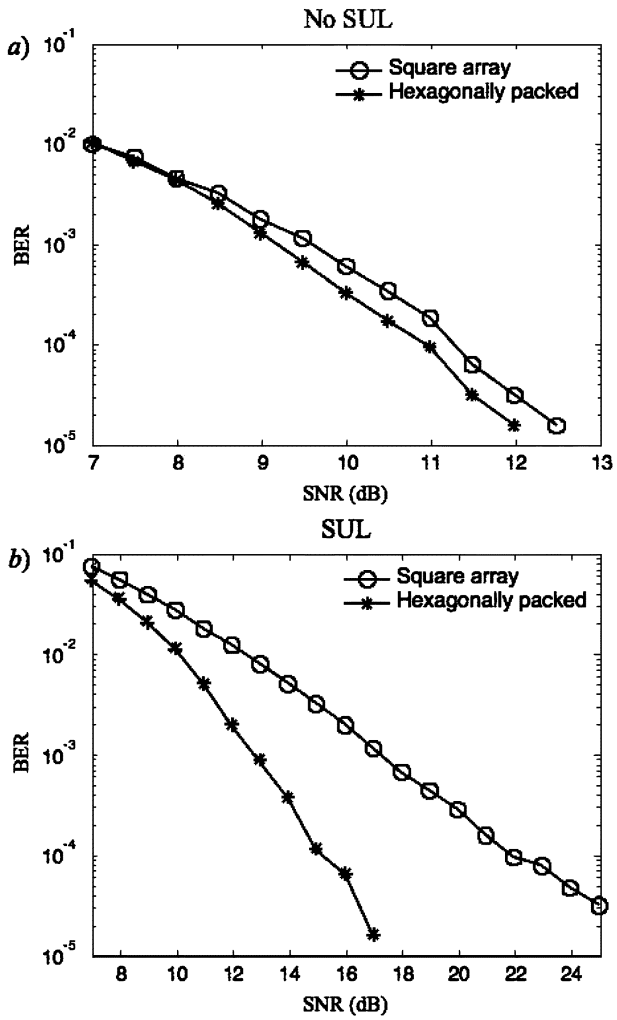

Fig. 9. Channel performance for different island distributions, for the case of (a) no SUL, and (b) an SUL present.

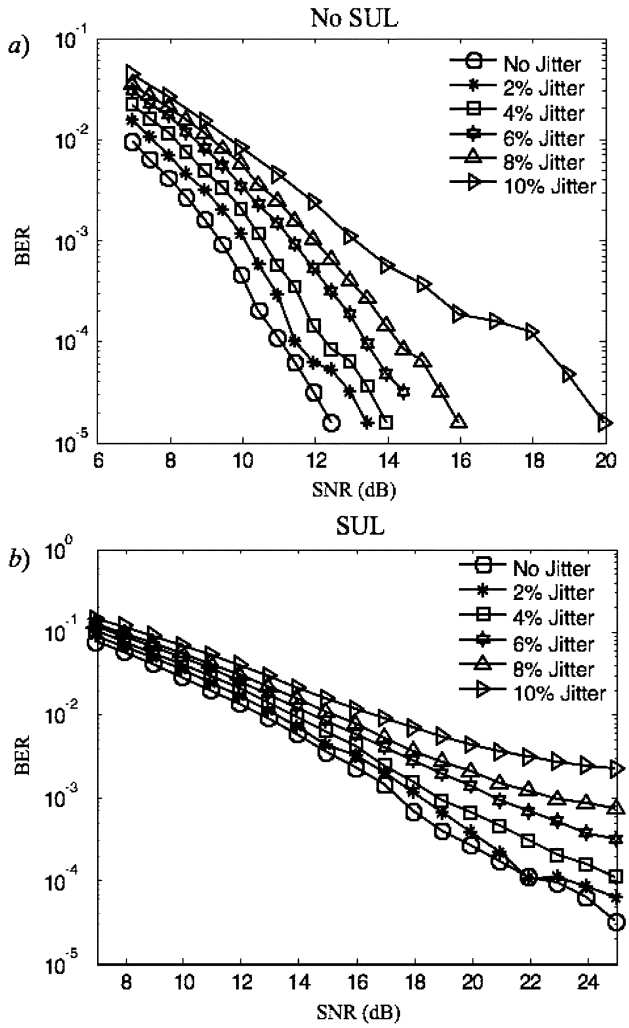

Fig. 10. Channel performance with varying amounts of lithography jitter, for the case of (a) no SUL, and (b) an SUL present.

is observed as the thickness of the recording medium is increased; particularly for the case of a patterned medium with an SUL. In both cases, the reduction in channel performance can be attributed to the increase in the pulsewidth as the film thickness is increased, particularly at the edges of the pulse response [10]. Generally, optimum channel performance is observed when a thin film, in this case $\delta = 10$ nm, is used. The result is sensible due to the need for thin films in continuous media in order to achieve sharp transitions and confirms conclusions drawn elsewhere [29] that in the patterned medium the film thickness should be of the order of the island spacing.

F. Jitter Analysis

As stated previously, the main source of noise in patterned media will be due to imperfections in the patterning process; this manifests itself as variations in island size and position that can be treated as being Gaussian in nature [18].

Fig. 10 illustrates the channel BER performance when lithography jitter is introduced as a random transition shift in the step superposition process. Here the jitter is specified as a percentage of the island period, $x_b = 25$ nm, along-track only.

In both cases, it is evident that the channel performance is significantly affected by the presence of lithography jitter. It is clear that the channel BER performance declines by an order of magnitude when more than 6% lithography jitter is introduced for the no SUL medium at a SNR of 12 dB; this corresponds to a jitter of $\sigma = 1.5$ nm, which indicates that tight tolerances on allowable island jitter may limit the attainable BER performance in future patterned media based storage systems.

V. Conclusion

Using a 3-D model of the replay process in patterned magnetic media storage, which enables signal contributions due to adjacent tracks to be included in the generation of the replay waveform, we have investigated how the characteristics of the geometrically constrained patterned media affects the performance of the read channel. Such an analysis may be useful for media designers who may be able to tailor the characteristics of the patterned medium to the benefit of read channel performance.

It has been shown that the best channel performance is observed when adopting a GPR target irrespective of whether an SUL is present (although acceptable BER performance is observed using the PR4 and EPR4 targets).

A number of media characteristics have been investigated using the particular GMR read sensor dimensions adopted. Key

conclusions that may be drawn show that a patterned medium with no SUL offers overall better BER performance compared to a patterned medium employing an SUL. In addition, ITI has a dramatic effect on the performance of the read channel for a patterned medium with an SUL. However, this performance may be improved significantly by using a hexagonally packed media.

In terms of island shape, no observable difference is evident between the BER performance using square or circular islands at the storage density of interest. However, increasing the width of the island has a detrimental effect on the BER performance of the read channel. Generally, reducing the island width below half the island period, $x_b/2$, has little appreciable effect of the channel performance. An increased island period leads to an improved channel performance, as expected. A reduced island period results in the degradation of the channel performance due to the increased amount of ISI and ITI in the replay waveform. However, in the case of a patterned medium with no SUL, the island period can be reduced from 25 to 20 nm, giving a storage density of 1.6 Tb/in^2, while still maintaining a BER performance comparable to the SUL case at 1 Tb/in^2. It is important to emphasize that the work presented here is not exhaustive and is presented only for fixed GMR read head dimensions. A full system optimization, including GMR reader geometry and write analysis, may modify the results presented and the conclusions made.

Overall, the channel BER performance in patterned media storage systems is strongly dependent upon the shape, size, period, and distribution of the islands. In particular, the read channel is especially sensitive to the presence of lithography noise, which manifests itself as jitter in the replay waveform. This will be a particular concern in the realization of a practical system based on patterned media, especially at higher storage densities where tighter tolerances on the patterning process may be required.

ACKNOWLEDGMENT

This work was supported by Engineering & Physical Sciences Research Council (EPSRC) under Grant GR/R63479. The authors extend their gratitude to Dr. D. Wilton and Dr. H. Shute of the Centre for Research in Information Storage Technology & the School of Mathematics & Statistics, the University of Plymouth, Plymouth, U.K., for their help and advice and for producing the 3-D potential distributions required for the replay modeling.

REFERENCES

[1] H. N. Bertram and M. Williams, "SNR and density limit estimates: A comparison of longitudinal and perpendicular recording," *IEEE Trans. Magn.*, vol. 36, no. 1, pp. 4–9, Jan. 2000.

[2] H. Sawaguchi, Y. Nishida, H. Takano, and H. Aoi, "Performance analysis of modified PRML channels for perpendicular recording systems," *J. Magn. Magn. Mater.*, vol. 235, pp. 265–272, 2001.

[3] S. Y. Chou, P. R. Krauss, and L. Kong, "Nanolithographically defined magnetic structures and quantum magnetic disk," *J. Appl. Phys.*, vol. 79, pp. 6101–6106, Apr. 1996.

[4] R. Wood, J. Miles, and T. Olson, "Recording technologies for terabit per square inch systems," *IEEE Trans. Magn.*, vol. 38, no. 4, pp. 1711–1718, Jul. 2002.

[5] M. H. Kryder and R. W. Gustafson, "High-density perpendicular recording-advances, issues, and extensibility," *J. Magn. Magn. Mater.*, vol. 287, pp. 449–458, Feb. 2005.

[6] S. Y. Chou, "Patterned magnetic nanostructures and quantized magnetic disks," *Proc. IEEE*, vol. 85, no. 4, pp. 652–671, Apr. 1997.

[7] R. L. White, R. M. H. New, and R. F. W. Pease, "Patterned media: A viable route to 50 Gbit/in^2 and up for magnetic recording?," *IEEE Trans. Magn.*, vol. 33, no. 1, pp. 990–995, Jan. 1997.

[8] R. L. White, "The physical boundaries to high-density magnetic recording," *J. Magn. Magn. Mater.*, vol. 209, pp. 1–5, 2000.

[9] S. H. Charap, P.-L. Lu, and Y. He, "Thermal stability of recorded information at high densities," *IEEE Trans. Magn.*, vol. 33, no. 1, pp. 978–983, Jan. 1997.

[10] P. W. Nutter, D. McA. McKirdy, B. K. Middleton, D. T. Wilton, and H. A. Shute, "Effect of island geometry on the replay signal in patterned media storage," *IEEE Trans. Magn.*, vol. 40, no. 6, pp. 3551–3558, Nov. 2004.

[11] G. F. Hughes, "Read channels for patterned media," *IEEE Trans. Magn.*, vol. 35, no. 5, pp. 2310–2312, Sep. 1999.

[12] ——, "Patterned media write designs," *IEEE Trans. Magn.*, vol. 36, no. 2, pp. 521–527, Mar. 2000.

[13] ——, "Read channels for prepatterned media with trench playback," *IEEE Trans. Magn.*, vol. 39, no. 5, pp. 2564–2566, Sep. 2003.

[14] ——, "Patterned media," in *The Physics of Ultra-High-Density Magnetic Recording*, M. L. Plumer, J. van Ek, and D. Weller, Eds. Heidelberg, Germany: Springer-Varlag, 2001, ch. 7.

[15] R. I. Potter, "Digital magnetic recording theory," *IEEE Trans. Magn.*, vol. MAG-10, no. 3, pp. 502–508, Sep. 1974.

[16] J. J. M. Ruigrok, *Short-Wavelength Magnetic Recording: New Methods and Analyses*. Oxford, U.K.: Elsevier Science, Apr. 1990, ch. 5.

[17] D. T. Wilton, D. McA. McKirdy, H. A. Shute, J. J. Miles, and D. J. Mapps, "Approximate three-dimensional head fields for perpendicular magnetic recording," *IEEE Trans. Magn.*, vol. 40, no. 1, pp. 148–156, Jan. 2004.

[18] M. M. Aziz, C. D. Wright, B. K. Middleton, H. Du, and P. Nutter, "Signal and noise characteristics of patterned media," *IEEE Trans. Magn.*, vol. 38, no. 5, pp. 1964–1966, Sep. 2002.

[19] Z. Jin, H. N. Bertram, and P. Luo, "Simulation of servo position error signal in perpendicular recording," *IEEE Trans. Magn.*, vol. 37, no. 6, pp. 3977–3980, Nov. 2001.

[20] J. Moon and W. Zeng, "Equalization for maximum likelihood detectors," *IEEE Trans. Magn.*, vol. 31, no. 2, pp. 1083–1088, Mar. 1995.

[21] H. Sawaguchi, Y. Nishida, H. Takano, and H. Aoi, "Performance analysis of modified PRML channels for perpendicular recording systems," *J. Magn. Magn. Mater.*, vol. 235, pp. 265–272, 2001.

[22] P. Kovintavewat, I. Ozgunes, E. Kurtas, J. R. Barry, and S. W. McLaughlin, "Generalized partial-response targets for perpendicular recording with jitter noise," *IEEE Trans. Magn.*, vol. 38, no. 5, pp. 2340–2342, Sep. 2002.

[23] S. X. Wang and A. M. Taratorin, *Magnetic Information Storage Technology*. San Diego, CA: Academic, 1999, ch. 12.

[24] H. Ide, "A modified PRML channel for perpendicular recording," *IEEE Trans. Magn.*, vol. 32, no. 5, pp. 3965–3967, Sep. 1996.

[25] J. Chen and J. Moon, "Detection signal-to-noise ratio versus bit cell aspect ratio at high areal densities," *IEEE Trans. Magn.*, vol. 37, no. 3, pp. 1157–1168, May 2001.

[26] S. Batra, J. D. Hannay, H. Zhou, and J. S. Goldberg, "Investigations of perpendicular write head design for 1 Tb/in^2," *IEEE Trans. Magn.*, vol. 40, no. 1, pp. 319–325, Jan. 2004.

[27] P. W. Nutter, H. Du, V. Vorithitikul, D. Edmundson, E. W. Hill, J. J. Miles, and C. D. Wright, "Fabrication of patterned Pt/Co multilayers for high density probe storage," in *Inst. Elect. Eng. Proc. Sci. Technol.*, vol. 150, Sep. 2003, pp. 227–231.

[28] P. W. Nutter, I. T. Ntokas, B. K. Middleton, and D. T. Wilton, "Effect of island distribution on error rate performance in patterned media," *IEEE Trans. Magn.*, vol. 41, no. 10, pp. 3214–3216, Oct. 2005.

[29] B. D. Terris and T. Thomson, "Nanofabricated and self-assembled magnetic structures as data storage media," *J. Phys. D, Appl. Phys.*, vol. 38, pp. R199–R222, Jun. 2005.

Manuscript received January 22, 2005; revised August 11, 2005.